ISSN 1975-8359(Print) / ISSN 2287-4364(Online)
The Transactions of the Korean Institute of Electrical Engineers Vol. 67, No. 7, pp. 981~986, 2018
http://doi.org/10.5370/KIEE.2018.67.7.981

아크유도형 DC 차단기의 동작 특성

Operating Characteristics of Arc-induction Type DC Circuit Breaker

박 상 용* · 최 효 상†
(Sang-Yong Park · Hyo-Sang Choi)

Abstract - AC(alternating current) CB(circuit breaker) at the fault occurred in the existing AC distribution system is limiting the fault current through zero cross-point. However, DC(direct current) CB does not have zero cross-point. Therefore, arc occurred by on-off operation of DC CB is very huge. Nowadays, many research team are studying the way to decrease breaking time, which is one of the essential conditions in DC CB. We suggested novel arc-induction type DC CB in this paper. The proposed arc-induction type DC CB is composed of the mechanical Arc ring and DC CB. We confirmed the operation of arc-induction type DC CB through the HFSS(High Frequency Structure Simulator) 3D simulation program and performed the experiment for operation characteristics. Results showed that arcing time of the arc-induction type DC CB by using induction ring was faster than existing mechanical DC CB. On the transient system, we confirmed stable operation characteristics of the arc-induction type DC CB through the simulation and experimental results. We expect that the proposed arc-induction type DC CB technology is will go to stay ahead of the existing DC CB technology.

Key Words : Induction ring, Arc-induction type, DC Circuit breaker, Mechanical Circuit Breaker

1. Introduction

In this study, an arc-induction type DC CB(circuit breaker), which induces an arc by connecting an induction needle to the mechanical DC CB, was proposed. Devised based on the principle of the lightning rod, the induction needle is placed near the mechanical contact point. The arc generated in the breaker is then guided to the induction needle to extinguish the arc stably. To develop an arc-induced DC CB, its breaking behavior characteristics were analyzed through the high frequency structure simulation (HFSS) 3D electromagnetic field analysis program and a prototype experiment[1-4].

2. Background

2.1 Coulomb's law and electric field analysis criteria

In Equation (1), F stands for an electrical force, and K represents the Coulomb's law constant, which is a proportional constant. As the arc-induction type DC CB operation in the air, a $9.0\times10^9 N\cdot m^2/c^2$ air constant is applied, where and each represents the amount of charge at different points while F represents the distance between, Q_1 and Q_2.

The electric field E is a space in which an electric force is engaged and to which an electric charge is applied. Assuming that the force received when the positive charge q of one point is placed in the electric field is F, the intensity of the electric field at that point can be derived as shown in Equation (3). The intensity of an electric field is the magnitude of the force received by the unit charge, and the direction signifies the direction of the force received by the positive charge. The power of charge q can be expressed as Equation (4) according to Coulomb's law. The electric field at a random point can be expressed by Equations (5) and (6) because it is the force received by the unit charge. Therefore, the arc induction phenomenon can be verified based on electric field analysis.

$$F=\frac{k\cdot Q_1\cdot Q_2}{d^2} \tag{1}$$

$$F=(9.0\times10^9 N\cdot m^2/C^2)\cdot Q_1\cdot Q_2/d^2 \tag{2}$$

$$E=\frac{F}{q}[N/C, V/m] \tag{3}$$

† Corresponding Author : Dept. of Electric Engineering, Chosun University, Korea.
E-mail: hyosang@chosun.ac.kr
* Dept. of Electric Engineering, Chosun University, Korea.
Received : March 8, 2018; Accepted : June 29, 2018

$$F = \frac{1}{4\pi\varepsilon_0} \times \frac{Qq}{r^2} \quad (4)$$

$$E = \frac{F}{q} \quad (5)$$

$$E = \frac{1}{4\pi\varepsilon_0} \times \frac{Q}{r^2} \quad (6)$$

3. Operation Principle and Mechanism of the Arc-induction type DC DB

3.1 Operation principle

Fig. 1 shows the operation principle of the arc-induction type DC CB. Fig. 1(a) represents a fixed pole Anode, Fig. 1(b) a movable pole Cathode, and Fig. 1(c) an induction needle. The induction needle is placed directly above the Anode. The reason for this is as follows.

- The charge (-) moving along the equipotential surface of the conductors performs zero work.
- The equipotential surface always intersects the electric force line perpendicularly.
- As the radius of curvature of the conical shape smaller than that of the cylindrical shape enables the concentration of charges, the electric field is strong.

Fig. 1(d) represents the induction gap, which is fixed at 2 mm. Fig. 1(e), on the other hand, represents the polar gap, which changes depending on the movable pole Cathode.

3.2 Mechanism

At the steady state, the polar gap is zero, and the Anode and Cathode have closed. The steady current flows to the load without the resistance by the induction needle, which has separated by a specific distance. The arc induction mechanism of the induction needle in the case of an accident could be explained in three steps using Coulomb's law.

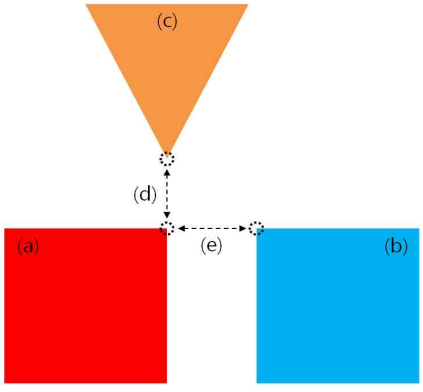

Fig. 1 The principle of Arc-induction type DC CB

First, when polar gap is less than induction gap, the Cathode moves opposite the Anode and block the fault current. The arc occurs between the Anode with a relatively small d value and the Cathode.

Second, when polar gap is equals to induction gap, the polar gap increases as the Cathode moves. Therefore, the electric force F decreases.

Third, when polar gap is more than induction gap and the Cathode has fully moved. The arc has fully absorbed and induced by the induction needle. This was because the electrical force F between the Anode and the induction needle was relatively stronger than the electrical force F between the Anode and the Cathode.

4. Simulation

4.1 HDSS simulation

We designed a simulation model of an arc-induction type DC CB using the HFSS electromagnetic field analysis program. The breaker section has constructed based on the above structure. The parameters of the configured Anode, Cathode, induction needle, induction ring, and ground wire have shown in Table 1.

4.1 HDSS simulation results and discussion

In this study, HFSS 3D simulation analysis has performed

Table 1 Parameters of the simulation design condition (breaking part)

Name	Standards	Value
Anode Cathode	Material	Cooper(Cu), Plating silver(Ag)
	Diameter	10 mm
	Height	15 mm
Induction needle	Material	Cooper(Cu), Plating silver(Ag)
	Diameter(bottom)	10 mm
	Height	25 mm
Induction ring	Material	Cooper(Cu), Plating silver(Ag)
	Diameter(inside)	70 mm
	Diameter(outside)	80 mm
	Width	10 mm
	Thickness	5 mm
Ground wire	Material	Cooper(Cu)
	Length	90 mm
	Width	12 mm
	Thickness	0.5 mm

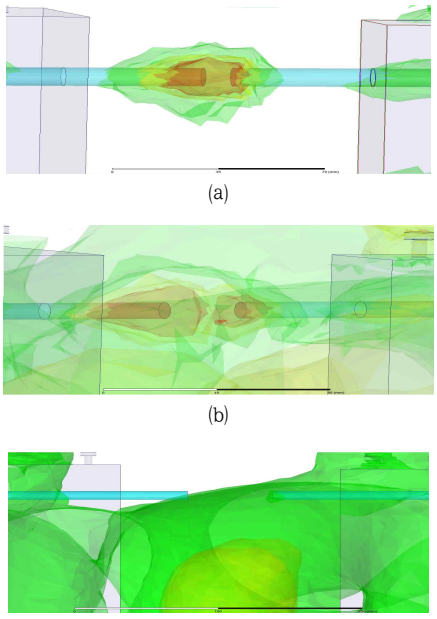

Fig. 2 The magnitude of the electric field generated at the mechanical contact points when there was no induction needle, (a) 5 mm, (b) 30 mm, (c) 60 mm

to confirm the arc induction of the arc-induction type DC CB. Fig. 2 shows the magnitude of the electric field generated at the mechanical contact point when there was no induction needle. Fig. 2(a) shows the electric field when the gap between the contact points was 5 mm. It can has confirmed that the strongest electric field has generated between the two contact points placed at 5 mm intervals. Fig. 2(b) shows the electric field distribution when the gap between the contact points was 30 mm. It could had confirmed that a relatively strong electric field has still being generated between the two contact points. Fig. 2(c) shows the electric field distribution when the gap between the contact points was 60 mm. It could had confirmed that a large electric field continuously has generated at the contact points. Fig. 3 shows the electric field generated is at the contact points when the induction ring has applied. Fig. 3(a) shows the electric field distribution when the gap between the contact points was 5 mm. It can has seen that a strong electric field generated at the two contact points. Fig. 3(b) shows the electric field when the gap between the contact points was 30 mm. It can has seen that the electric field distributed between the two contact points. This could had confirmed that the electric field also has distributed in the induction ring, thereby confirming that there was also an electric charge in the induction ring. Fig. 3(c) shows the electric field when the gap between the contact points was

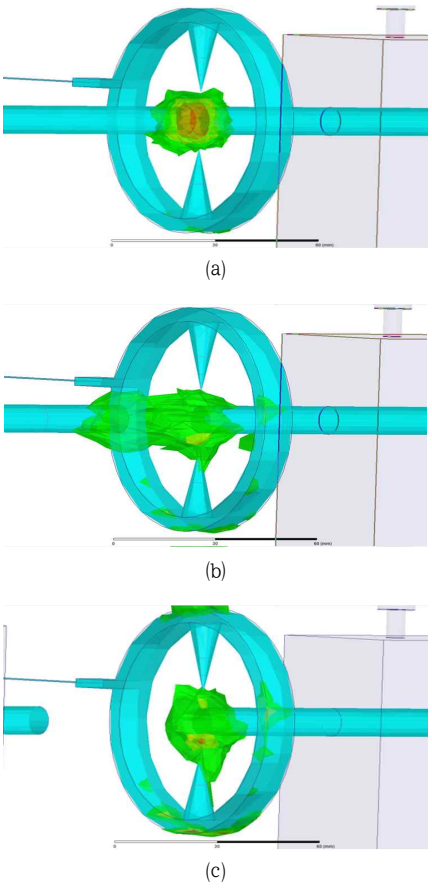

Fig. 3 The electric field generated at the contact point when the induction ring has applied, (a) 5 mm, (b) 30 mm, (c) 60 mm.

60 mm. It could had confirmed that the electric field had not generated in the Cathode whereas it had generated in the Anode and the induction ring, respectively, this was because the gap between the Anode and the Cathode increased, thereby weakening the electric field. Figs. 2 and 3 show that the value of the electric field generated at the contact points have changed depending on the presence or absence of an induction needle. When the gap between the Anode and the Cathode has increased, the electric field has generated from the induction needle, this was because the induction needle can absorb the arc when it occurred.

Fig. 4 is a graph showing the electric field distribution between the contact points according to the presence or absence of an induction needle, which calculated using Equation (6). When there was no induction needle, a field ratio of up to 242 % occurred. On the contrary, when there was the induction needle, the maximum field ratio of up to 103 % occurred. Therefore, it could had confirmed that the intensity of the electric field has significantly reduced by

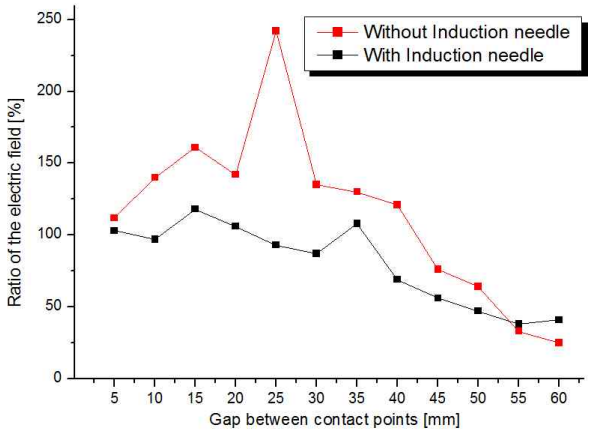

Fig. 4 Electric field distribution between the contact points according to the presence or absence of an induction needle

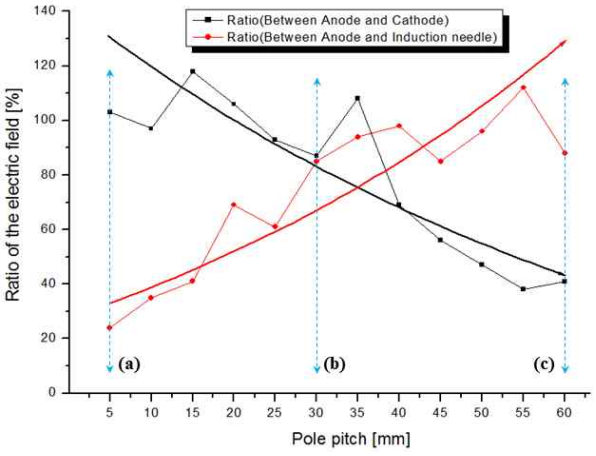

Fig. 5 The graph of the ratio of electrical field calculated according to the contact points (a) 5 mm, (b) 30 mm, (c) 60 mm

the presence of an induction needle. Fig. 5(a), (b), and (c) show the electric field ratios at the polar gaps of 5, 30, and 60 mm, respectively. The electric field ratio calculated using Equations (7) and (8). The electric field ratio between the Anode and the Cathode have gradually lowered as the polar gap increased, this was because the electric force between the contact points have weakened by the increase in the gap in accordance with Coulomb's law.

$$\text{Anode \& Cathode Ratio(E)} = \frac{Cathode}{Anode} \times 100 \tag{7}$$

$$\text{Anode \& needle Ratio(E)} = \frac{Induction\ needle}{Anode} \times 100 \tag{8}$$

The field ratio between the Anode and the induction needle gradually increased as the polar gap increased, this was because the force acting between the charges become smaller as the gap between the Anode and the Cathode increases. Conversely, the growing of force acting between the Anode and the induction needle and increase the intensity of the electric field.

5. Experimental

5.1 Experimental setup

Fig. 6 shows an experimental equivalent circuit diagram of the arc-induction type DC CB. The primary line consists of DC power supply and mechanical contact points, an Anode, a Cathode, and a load connected in series. The secondary line consists of the induction needle, induction ring, and ground wire connected in series and parallel. 20 V and 100 A had applied, respectively, using DC power supply. The circuit voltage and current flow had measured using an oscilloscope while a pneumatic cylinder had used to open the contact point. The air pressure had used in the pneumatic cylinder was 907.69 mm/s on average at an air pressure of 8 kPa. The load resistance of the circuit was 0.2 Ω.

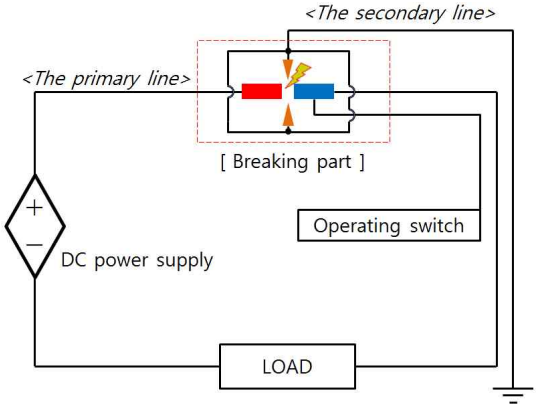

Fig. 6 An equivalent circuit diagram of Arc-Induction type DC CB for the experiment.

5.1 Experimental results

Fig. 7 shows an actual arc-induction type DC CB. Fig. 7(a) shows the fabricated arc induction needle. Fig. 7(b) shows the arc generated when the contact points have opened as voltage is applied through the power supply. Fig. 8(a) shows

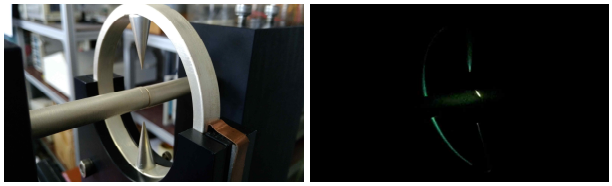

(a) (b)

Fig. 7 An actual arc-induction type DC CB, (a) The fabricated arc induction needle, (b) The actual arc.

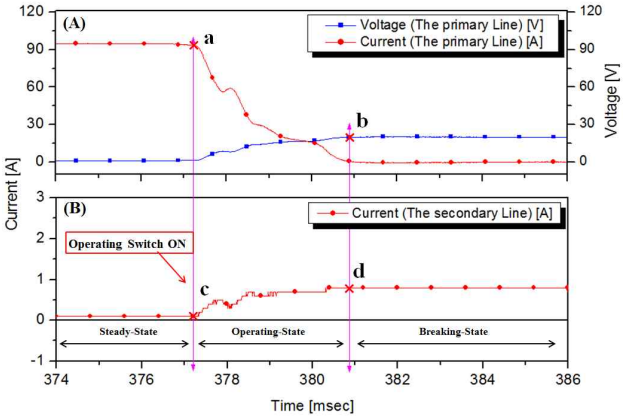

Fig. 8 An experimental data according to the interruption behavior of the arc-induction type DC CB

an experimental data according to the interruption behavior of the arc-induction type DC CB. When the Anode and Cathode contact points have connected, the voltage was about 0 V and the current was about 94.2 A. As the operating switch has turned on, the voltage rose from about 0 V to about 20.8 V while the current dropped from about 94.2 A to about 0 A. Fig. 8(b) shows the current generated from the arc induction needle. Normally, about 0 A flowed, but thereafter, about 0.2 A flowed immediately after the accident, and about 1 A when the CB completed its operation. Although the applied current voltage was low and the generated arc was insufficient, it could had confirmed that the arc was induced by the induction needle.

6. Conclusions

In this study, a new arc induction method designed to improve the operational reliability of the DC distribution system has proposed. The arc induction phenomenon of the DC CB using an induction needle was analyzed through simulation and an experiment.

The simulation modeling was implemented using the HFSS 3D electromagnetic field analysis program while the current flow has analyzed based on the field distribution phenomenon and the electric field ratio, which change with the polar gap. A clear difference in the flow of the electric field according to the presence or absence of an induction needle was confirmed. Therefore, it was verified that the arc generated between the contact points could have absorbed and induced by the induction needle. The experimental results of the arc-induction type DC CB based on simulation modeling is confirmed the voltage and current change according to the arc shape and the state variation that occurs in the breaker section as a prototype model. In this study, the arc induction phenomenon was confirmed in the DC CB using an induction needle. There is continuously a plan to study the arc induction phenomenon in the future by constructing a high capacity DC power supply and other necessary equipment.

Acknowledgement

"This work was supported by the National Research Foundation of Korea(NRF) grant funded by the Korea government(MSIT) (No.2018R1A2B2004242)."

References

[1] F. M. Uriarte, A. L. Gattozzi, J. D. Herbst, H. B. Estes, T. J. Hotz, A. Kwasinski and R. E. Hebner, “A DC arc model for series faults in low voltage microgrids”, *IEEE Trans. Smart Grid*, vol. 3, no. 4, pp. 2063-2070, 2012.

[2] S. M. Lee, “A study on low-voltage DC circuit breakers”, *IEEE ISIE Conf*, Taiwan, pp. 1-6, 2013.

[3] Z. Ganhao, “Study on DC circuit breaker”, *Fifth International Conference on Intelligent Systems Designs and Engineering Applications (ISDEA)*, Human, China, pp. 942-945, 2014.

[4] Z. He, J. Hu, L. L and R. Zeng, “Mechanical DC circuit breakers and FBSM-based MMCs in High-Voltage MTDC Network: Coordinated Operation for Network Riding Through DC Fault”, International Conference on RPG 2015, pp. 1-6, 2015.

저 자 소 개

박 상 용 (Sang-Yong Park)

1988년 08월 14일 생. 2016년 조선대 전기공학과 졸업(학사). 2018년 동 대학원 졸업(공학석사). 2014~현재 동 대학원 박사과정.
Tel : 062-230-7054
E-mail : sangyong4400@gmail.com

최 효 상 (Hyo-Sang Choi)

1966년 2월 21일 생. 1989년 전북대 전기공학과 졸업(학사). 1994년 동 대학원 전기공학과 졸업(공학석사). 2000년 동 대학원 전기공학과 졸업(공학박사). 현재 조선대 전기공학과 교수, 시민 르네상스 평생교육원 원장, 미래사회융합대학 학장
Tel : 062-230-7025
E-mail : hyosang@chosun.ac.kr